Free fatty acids induce coronary microvascular dysfunction via inhibition of the AMPK/KLF2/eNOS signaling pathway

YANDA ZHANG*, JIAN ZHAO*, CHANGZHEN REN, BOWEN HU, RU DING, ZHIQING HE and CHUN LIANG

Department of Cardiology, Second Affiliated Hospital of Naval Medical University, Shanghai 200003, P.R. China

Received October 14, 2022; Accepted January 26, 2023

DOI: 10.3892/ijmm.2023.5237

Abstract. Increased levels of serum free fatty acids (FFAs) are closely associated with microvascular dysfunction. In our previous study, a coronary microvascular dysfunction (CMD) model was successfully established via lipid infusion to increase the levels of serum FFAs in mice. However, the underlying mechanisms remained poorly understood. Therefore, the aim of the present study was to explore the mechanism underlying FFA-induced CMD. A CMD mouse model was established via lipid combined with heparin infusion for 6 h to increase the concentration of serum FFAs. Following the establishment of the model, the coronary flow reserve (CFR), extent of leukocyte activation and cardiac microvascular structures were assessed in the mice. Cardiac microvascular endothelial cells (CMECs) were treated with different concentrations of palmitic acid and cell viability was evaluated. Changes in the expression levels of AMP-activated protein kinase (AMPK), Krüppel-like factor 2 (KLF2) and endothelial nitric oxide synthase (eNOS) were identified by immunohistochemical and western blot analyses. Experiments using AMPK activator, KLF2 overexpression plasmid, small interfering RNAs and nicorandil were subsequently designed to investigate the potential involvement of the AMPK/KLF2/eNOS signaling pathway. These experiments revealed that FFAs could induce CMD in mice, which was characterized by reduced CFR (1.89±0.37 vs. 2.74±0.30) and increased leukocyte adhesion (4,350±1,057.5 vs. 11.8±5.4 cells/mm^2) compared with the control mice. CD11b expression and intracellular reactive oxygen species (ROS) levels were increased in CMD model mice compared with control mice. Serum TNF-α and IL-6 levels were higher in the model group than in the control group. Transmission electron microscopy revealed that CMECs in heart tissues of model mice were severely swollen. In addition, palmitic acid decreased CMEC viability and increased ROS production in a dose-dependent manner. Notably, the AMPK/KLF2/eNOS signaling pathway was demonstrated to be suppressed by FFAs both *in vivo* and *in vitro*. Activation of this axis with AMPK activator, KLF2 overexpression plasmid or nicorandil restored the CFR in CMD model mice, inhibited oxidative stress and increased CMEC viability. Taken together, the results of the present study demonstrated that FFAs could induce CMD via inhibition of the AMPK/KLF2/eNOS signaling pathway, whereas activation of this pathway led to the alleviation of FFA-induced CMD, which may be a therapeutic option for CMD.

Introduction

Ischemic heart disease (IHD) is a leading cause of morbidity and mortality, affecting 112 million individuals worldwide in 2015 (1). As one of the main causes of IHD, coronary microvascular dysfunction (CMD) accounts for approximately two-thirds of clinical conditions presenting with symptoms and signs of myocardial ischemia without obstructive coronary disease, including microvascular angina and myocardial infarction with non-obstructive coronary artery disease (2). Although CMD has a high prevalence in IHD and is associated with adverse outcomes, the diagnosis of CMD remains challenging and the underlying mechanisms remain poorly understood (3). It has been previously demonstrated that endothelial dysfunction, oxidative stress, inflammation and other factors may be involved in the development of CMD (4). At present, treatment options for CMD are mainly focused on exploring anti-inflammatory and anti-anginal pathways (5).

Higher serum free fatty acid (FFA) levels are often observed in patients with cardiovascular disease and these are associated with recurrence and poor prognosis (6-8). Previous studies have demonstrated that a high level of serum FFAs is an independent risk factor for cardiovascular disease (9,10). This association is more pronounced in diabetes due to impaired glucose utilization (11). An excessive FFA oxidation rate causes abnormal energy metabolism and myocardial dysfunction in diabetic patients (12,13). In addition, high FFAs levels have been reported to promote lipid accumulation and lipotoxicity in cardiomyocytes, which contributes to systemic inflammation, oxidative stress and eventual cardiomyocyte

Correspondence to: Dr Chun Liang, Department of Cardiology, Second Affiliated Hospital of Naval Medical University, 415 Fengyang Road, Huangpu, Shanghai 200003, P.R. China
E-mail: chunliang@smmu.edu.cn

*Contributed equally

Key words: coronary microvascular dysfunction, free fatty acids, AMP-activated protein kinase, Krüppel-like factor 2, endothelial nitric oxide synthase, nicorandil

apoptosis (14,15). Our previous study demonstrated that a CMD mouse model could be successfully established via lipid emulsion infusion, which resulted in an increase in the serum FFA level (16). However, the underlying mechanism remained unclear. AMP-activated protein kinase (AMPK) is an essential component of the adaptive response to cardiomyocyte stress that occurs during myocardial ischemia (17). AMPK modulates fatty acid metabolism in the ischemic heart, and activated AMPK appears to be protective in reducing myocardial necrosis during ischemia-reperfusion (18). Its activation has also been revealed to improve exercise performance and peripheral vascular insufficiency in mice fed on a high-fat diet (19). AMPK also regulates the downstream transcription factor, Krüppel-like factor 2 (KLF2), which is expressed in endothelial cells and has the role of preserving various endothelial functions (20).

The AMPK/KLF2 axis activates the expression of endothelial nitric oxide (NO) synthase (eNOS) in endothelial cells, subsequently promoting the release of vasodilator-NO (21). Endothelial cell-derived NO serves key roles in vasodilation, inhibition of platelet aggregation and reduction of leukocyte adhesion, and as an antioxidant (22). Activation of the AMPK/KLF2/eNOS signaling pathway has been demonstrated to improve endothelial dysfunction and slow down the progression of atherosclerosis, pulmonary arterial hypertension and other diseases (23-25).

Cardiac microvascular endothelial cells (CMECs) serve a key role in maintaining normal coronary circulation (26). A previously published study suggested that a high-fat diet could inhibit AMPK expression (27), thus we hypothesized that the AMPK pathway may be involved in the detrimental effects of FFAs on CMECs.

Therefore, the aim of the present study was to explore the AMPK/KLF2/eNOS signaling axis both *in vivo* (in a CMD mouse model established by lipid infusion) and *in vitro* [in CMECs treated with palmitic acid (PA)], and to investigate the underlying mechanism.

Materials and methods

Animals and reagents. A total of 45 C57BL/6J mice (male; 6-8 weeks old; weight, 20±2 g) were obtained from the Shanghai Jihui Laboratory Animal Care Co., Ltd. All mice were housed individually and were maintained at 22˚C with 40-60% humidity and a 12-h light/dark cycle starting at 6:00 am. The mice were fed with normal chow and had free access to food and water throughout the experiment. Nicorandil was purchased from Beijing Sihuan Kebao Pharmaceutical Co., Ltd. FFAs and reactive oxygen species (ROS) assay kits were obtained from Beijing Solarbio Science & Technology Co., Ltd. The anti-GAPDH antibody was obtained from Abcam, whereas the anti-KLF2 antibody was purchased from BIOSS, anti-p-eNOS antibody was purchased from Affinity Biosciences, and the anti-AMPK, anti-phosphorylated (p-)AMPK and anti-eNOS antibodies were obtained from Cell Signaling Technology, Inc. The lipid emulsion was purchased from Fresenius Kabi Huarui Pharmaceutical Co., Ltd. Anti-CD62L and anti-CD11b antibodies were purchased from BD Biosciences. Mouse interferon-γ (IFN-γ) ELISA kit (cat. no. F10660), mouse interleukin-6 (IL-6) ELISA kit (cat. no. F10830), mouse NO ELISA kit (cat. no. F11321), mouse superoxide dismutase (SOD) ELISA kit (cat. no. F11502) and mouse tumor necrosis factor-α (TNF-α) ELISA kit (cat. no. F11630) were obtained from Shanghai Xitang Biotechnology Co., Ltd. The AMPK activator, 5-aminoimidazole-4-carboxamide ribonucleotide (AICAR), was purchased from MedChemExpress. The Cell Counting Kit-8 (CCK-8) assay kit was obtained from Shanghai DODGEN Chemical Technology Co., Ltd. PA was obtained from Sigma-Aldrich; Merck KGaA. The KLF2 overexpression plasmid was obtained from Shanghai GeneChem Co., Ltd. Finally, Lipofectamine® 3000 transfection reagent was obtained from Thermo Fisher Scientific, Inc.

The entire animal experimental protocol used in the present study was carefully examined and approved by the Animal Experiment Ethics Committee of the Second Affiliated Hospital of Naval Medical University (approval no. 2020SL037; Shanghai, China). All animal care procedures were carried out in accordance with the Animal Research: Reporting of *In Vivo* Experiments guidelines on animal research (28).

Establishment of the CMD model. A total of 30 male C57BL/6J mice were randomly assigned to the control, model and nicorandil groups (n=10 mice in each group). Normal saline solution (200 μl once per day) was administered to the mice in the control and model groups via intraperitoneal (i.p.) injection for 3 days, whereas the mice in the nicorandil group were treated with an injection (i.p.) of nicorandil (200 μl nicorandil at a concentration of 1.95 mg/kg once per day for 3 days). Nicorandil, a drug for CMD, is used to stimulate the upregulation of eNOS (29) and was used in the present study to investigate the AMPK/KLF2/eNOS signaling pathway. As shown in Fig. 1A, the mice were subsequently anaesthetized with sodium pentobarbital (40 mg/kg), and the jugular vein was catheterized using a microcatheter. Afterwards, the mice underwent a 6-h infusion with either normal saline or lipid emulsion combined with heparin using a micro-pump (the lipid component was 20% Intralipid®; Fresenius Kabi Huarui Pharmaceutical Co., Ltd.; heparin was infused at a concentration 20 U/ml, and at a rate of 0.1 ml/h).

Coronary flow reserve (CFR) measurement. Following lipid infusion, the mice were immediately anaesthetized using isoflurane (3% for induction and 1-2.5% for maintenance). Hyperemic flow was achieved by increasing the percentage of isoflurane to 2.5%, whereas the baseline flow was achieved by reducing the isoflurane percentage to 1% (30). Data were measured using a Doppler signal processing workstation. The CFR was calculated according to the following formula: $CFR=P/R=V_{high}/V_{low.}$(where P is the peak blood flow, R is the resting blood flow, V_{high} is the hyperemic blood flow velocity and V_{low} is the baseline blood flow velocity).

Cremaster microcirculation assessment. Mice were anesthetized with sodium pentobarbital (40 mg/kg) immediately after the lipid infusion. Intravital microscopy (Olympus BX51 WI upright microscope; Olympus Corporation) was used to record the cremaster microvascular blood flow and leukocyte adhesion in venules. Leukocyte flux and leukocyte endothelium interactions (rolling and adhesion) analysis were conducted as

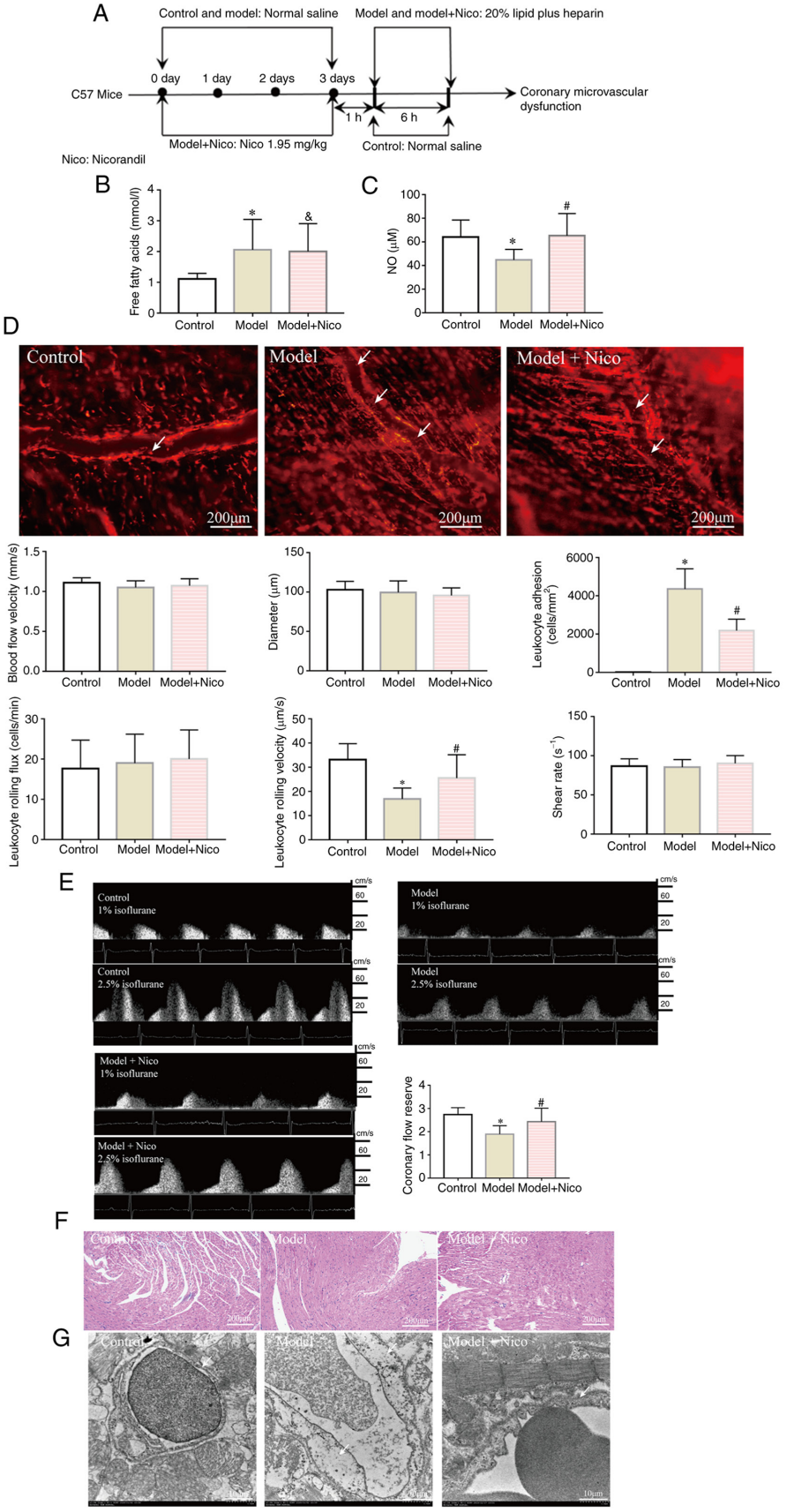

Figure 1. Lipid infusion induces CMD, whereas treatment with nicorandil improves CMD. (A) Flow chart of the protocol for the animal experiments. (B) Serum free fatty acid levels were increased in the Model and Model + Nico groups. (C) Serum NO levels were decreased in the Model group, whereas the NO levels were increased in the Model + Nico group. (D) Lipid infusion-activated leukocytes in cremaster microcirculation (white arrows indicate the leukocytes that adhered to the cremaster microvascular wall). Scale bar, 200 μm. (E) Coronary flow reserve was decreased in the Model group. (F) Images captured under a light microscope (magnification, x200; scale bar, 200 μm). (G) Edema of endothelial cells (white arrow; scale bar, 10 μm). Data are presented as the mean ± SD. *P<0.05, Model (n=10) vs. Control (n=10); $^{\#}$P<0.05, Model + Nico (n=10) vs. Model (n=10); $^{\&}$P<0.05, Model + Nico (n=10) vs. Control (n=10). CMD, coronary microvascular dysfunction; Nico, nicorandil; NO, nitric oxide.

described previously (31). Briefly, rolling leukocyte flux was measured at the indicated time points by counting the number of rolling leukocytes per 20 sec that passed a reference point in the microvessel and the number was then presented as units of cells/min. Leukocyte rolling velocity was calculated by the velocity of 10 leukocytes rolling along the endothelial cell lining (mm/sec) and leukocyte adhesion (defined as being stationary for 20 sec) was counted in 100-μm-long vascular segments, and presented as the number of adherent cells/mm^2. Diameters (in mm) were measured perpendicularly to the vessel path. Finally, the venular wall shear rate was calculated based on the Newtonian definition, according to the following formula: Wall shear rate (sec^{-1})=8 x [red blood cell velocity (μm·sec^{-1})/venular diameter (μm)] (32).

AICAR intervention. A total of 15 male mice were randomly assigned to control (n=5), model (n=5) and AICAR (n=5) groups. Normal saline solution (200 μl once per day) was administered to the mice in the control and model groups via i.p. injection for 3 days. Mice in the AICAR group were treated with 200 μl AICAR (concentration, 0.5 mg/g) by i.p. injection for 3 days prior to lipid infusion (once per day for 3 days). Subsequently, microvascular dysfunction was induced in the model and AICAR groups by lipid infusion as aforementioned. Cultured CMECs *in vitro* were treated with AICAR (500 μM) for 3 h at 37˚C, then 400 μM PA was added and cells were incubated at 37˚C for 24 h.

Heart histological examination and ultrastructural analysis. Mice were sacrificed by cervical dislocation while under anesthesia induced by an i.p. injection of 40 mg/kg pentobarbital, and respiratory arrest was used to confirm animal death. Fresh heart sections were fixed in 4% paraformaldehyde at room temperature for 24 h, embedded in paraffin and serial 5-μm-thick sections were prepared. Morphological analysis of cardiomyocytes and microvessels was subsequently performed using H&E staining. Then, the sections were stained with hematoxylin for 5 min at room temperature, then washed with running water for 5 min and differentiated in 1% acid alcohol for 10 sec at room temperature. The sections were then stained with 1% eosin for 1 min, washed with running water and dehydrated in increasing concentrations of alcohol (70, 80, 90 and 100%) and cleared in xylene. Finally, H&E staining was observed under a BX43 light microscope (Olympus Corporation).

For the immunohistochemical analysis of KLF2, eNOS and p-eNOS, fresh heart sections were fixed in 4% paraformaldehyde at room temperature for 24 h, embedded in paraffin and serial 5-μm-thick sections were prepared. The sections were dewaxed in xylene, then rehydrated in a descending alcohol series (hydrated in 100, 95 and 80% ethanol and water for 5 min each). Antigen retrieval was performed by pre-treatment of the slides in citrate buffer (pH 6.0) (cat. no. G1202; Wuhan Servicebio Technology Co., Ltd.) in a microwave (720 W heating) oven for 12 min. Thereafter, the slides were cooled to room temperature in deionized water for 5 min. The sections were incubated in 0.3% H_2O_2-methanol solution for 10 min and then washed with PBS three times. To block endogenous peroxidase activity, 50 μl peroxidase blocking solution was added to each section and these were incubated for 10 min at room temperature. Each section was then incubated with 50 μl 10% nonimmune goat serum (OriGene Technologies, Inc.) for 10 min at room temperature, rinsed with PBS and incubated with 50 μl primary antibody [KLF2 (dilution, 1:400; cat. no. bs-2772R; BIOSS), eNOS (dilution, 1:1,000; cat. no. GB12086; Wuhan Servicebio Technology Co., Ltd.) and p-eNOS (diluted 1:100; cat. no. AF3247; Affinity Biosciences)] at 4˚C overnight. The sections were then incubated with 50 μl secondary antibody [HRP conjugated goat anti-rabbit IgG (dilution, 1:200; cat. no. GB23303; Wuhan Servicebio Technology Co., Ltd.) or HRP-conjugated goat anti-mouse IgG (diluted 1:200; cat. no. GB23301; Wuhan Servicebio Technology Co., Ltd.)] at room temperature for 10 min. The reaction was developed with freshly prepared 3,3'-diaminobenzidine, and observed under a Leica DM4000 microscope (Leica Microsystems GmbH) for 3-10 min, with brown indicating positive staining. The slides were then counterstained with hematoxylin for 3 min at room temperature, washed with running water, and dehydrated in increasing concentrations of alcohol (75, 85 and 100%) and cleared in xylene. The pathological and immunohistochemical changes were evaluated and photographed under a BX43 light microscope (Olympus Corporation). Data analysis was performed using Multiplex IHC v2.2.0 module analysis software (Indica Labs, Inc.).

Heart samples were fixed in 2.5% glutaraldehyde in 0.1 mol/l cacodylate buffer at 4˚C overnight, fixed in 1% osmium tetroxide at 4˚C for 2 h and then embedded in Epon using an Embed-812 kit (Electron Microscopy Sciences) at room temperature overnight. Ultrathin sections (80-100 nm) were obtained from selected areas using an ultrathin microtome (Leica EM UC7; Leica Microsystems GmbH). The ultrathin sections of the cubes were stained with 3% uranyl acetate and lead citrate at 25˚C for 30 min. Then, the sections were examined using transmission electron microscopy (TEM; Tecnai™ G2 20; FEI; Thermo Fisher Scientific, Inc.).

ELISAs and measurements of plasma FFAs. Blood samples (100 μl) were collected from the tail-veins of the mice in heparin-containing tubes, and plasma was prepared after centrifugation at 4,500 x g for 10 min at room temperature. Subsequently, aliquots were stored at -80˚C until use. The levels of plasma biomarkers, including IFN-γ, IL-6, NO, SOD and TNF-α, were determined using ELISA kits (Shanghai Xitang Biotechnology Co., Ltd.). FFAs were measured using an FFA Content Assay Kit (cat. no. BC0595; Beijing Solarbio Science & Technology Co., Ltd.) was conducted according to the manufacturer's user guide. The preparation of reagent1 was accomplished following the ratio of n-heptane: absolute methanol: chloroform=24:1:25 at room temperature. The physical state of diphenylcarbazide was powder, absolute ethanol was added at the time of application and the liquid volume was 13 ml. The standard solution was chloroform-dissolved 5 μmol/ml palmitic acid solution. The microplate reader was preheated for 30 min, the wavelength was adjusted to 550 nm, and absolute ethanol was used as a blank (set to 0). Copper reagent was water-bathed at 37˚C for 30 min. Standard solution was diluted to 0.05, 0.1, 0.2, 0.4, 0.6, 0.8 and 1 μmol/ml with chloroform. Each 1.5-ml Eppendorf tube was first supplemented with 10 μl distilled water, sample, chloroform or standard solution. Then 100 μl reagent1 and 40 μl copper

reagent were added sequentially, followed by shaking for 10 min at room temperature and finally centrifugation at 850 g for 10 min at room temperature. A total of 50 μl of the supernatant was transferred to a 1.5-ml Eppendorf tube and 200 μl diphenylcarbazide was added, followed by shaking for 2 min and standing for 15 min at room temperature. Absorbance at 550 nm of each well of a 96-well plate was measured using a microplate reader (200 μl liquid volume was added per well). FFA concentrations were calculated for each plasma sample according to the standard curve.

Measurement of intracellular ROS in leukocytes and CMECs. The intracellular levels of ROS were measured by a fluorometric assay using the probe 2'-7'-dichlorodihydrofluorescin diacetate (DCFH-DA). Cells were resuspended in 2 ml PBS (10^6 cells/ml) and were subsequently incubated with 10 μM DCFH-DA at 37˚C for 20 min with continuous shaking. Cells were washed with PBS three times (2 min each at room temperature) and were transferred from a tube to a microplate prior to fluorescence being measured. To minimize the process of photo-oxidation, samples were stored in the dark. Finally, DCF fluorescence was measured using a microplate reader (488 nm excitation and 525 nm emission wavelengths).

Flow cytometric analysis of leukocytes. Blood (100 μl) was drawn from the great saphenous vein of the mice after lipid infusion. Ammonium chloride-potassium lysis buffer was used for erythrocyte removal. Blood samples were centrifuged at room temperature for 10 min at 850 x g, and the plasma was subsequently removed. Leukocytes were resuspended in 20 μl normal saline and then incubated with the appropriate antibodies as previously described (33). Phycoerythrin rat anti-mouse CD11b (cat. no. 557397) and allophycocyanin rat CD62L (cat. no. 5333152) antibodies (BD Biosciences) were diluted at a ratio of 1:5. Flow cytometry was performed using a Cytek DXP 8 Color upgraded BD FACS Calibur™ flow cytometer (BD Biosciences) by staining with appropriate antibodies, and the data were analyzed using FlowJo 10.0 software (Tree Star, Inc.).

Western blot analysis of heart tissue and CMECs. Heart tissue (50 mg) and CMECs were collected for quantitative analysis of the proteins. Proteins were extracted using RIPA lysis buffer [Hangzhou Multi Sciences (Lianke) Biotech Co., Ltd.]. Protein concentrations of heart tissues and CMECs were subsequently determined using a Takara Bradford Protein Assay kit (Takara Bio, Inc.). The proteins were diluted to a final protein concentration of 2.5 μg/μl in 1X loading buffer (Wuhan Servicebio Technology Co., Ltd.), and 25 μg protein was loaded onto each lane of the western blot gel (10%). After the proteins were separated, they were transferred to polyvinylidene fluoride membranes (Bio-Rad Laboratories, Inc.), which were blocked with 5% BSA (Shanghai Siding Biotechnology Co., Ltd.) for 2 h at room temperature. The membrane was incubated with the corresponding primary antibody overnight at 4˚C. The following day, HRP-labeled secondary antibodies (cat. no. 98164; Cell Signaling Technology, Inc.) were incubated with the membranes at room temperature for 2 h. The dilution of rabbit anti-KLF2 polyclonal antibody (cat. no. bs-2772R; BIOSS) was 1:300, and the dilution of rabbit anti GAPDH monoclonal antibody (cat. no. ab181602; Abcam) was 1:10,000. The dilution of rabbit anti-eNOS (cat. no. 32027; Cell Signaling Technology, Inc.), anti-AMPK (cat. no. 5832; Cell Signaling Technology, Inc.), anti-p-eNOS (Ser1177) (cat. no. AF3247; Affinity Biosciences) and anti-p-AMPK (Thr172) (cat. no. 50081; Cell Signaling Technology, Inc.) polyclonal antibody was 1:1,000. HRP-labeled secondary antibodies were used at a dilution of 1:5,000. All antibodies were diluted using TBS with 0.1% Tween-20 (Wuhan Servicebio Technology Co., Ltd.). Enhanced chemiluminescence western blotting substrate (Wuhan Servicebio Technology Co., Ltd.) was used to detect the immuno-reactive signals. The protein gray values were analyzed using ImageJ 1.6 software (National Institutes of Health).

Isolation and identification of CMECs. Primary mice CMECs were purchased from Saibaikang (Shanghai) Biotechnology Co., Ltd. and cultured in Complete™ Endothelial Cell Medium (ECM; Sigma-Aldrich; Merck KGaA) containing 10% FBS (ScienCell Research Laboratories. Inc.), 1% endothelial cell growth supplement and 1% penicillin/streptomycin at 37˚C in an atmosphere of 5% CO_2. CMECs were identified by immunofluorescence using an antibody against von Willebrand factor VIII, which is constitutively expressed on the surface of CMECs (34) (Fig. S1). In order to identify the CMECs, cells were seeded in 24-well plates ($2.0x10^4$ cells per well). The cells were then washed twice with PBS and fixed in ice-cold 100% methanol for 15 min at -20˚C. After rinsing with PBS three times for 5 min each, the samples were incubated with 0.1% Triton X-100 at room temperature for 10 min, blocked with 1% BSA at room temperature for 60 min, and incubated with rabbit anti-vWF polyclonal antibody (1:200; cat. no. 11778-1-AP; Proteintech Group, Inc.) at 4˚C overnight. The samples were then washed three times with PBS, followed by incubation with Alexa Fluor 488-conjugated secondary antibodies (1:500; cat. no. SA00006-2; Proteintech Group, Inc.) at room temperature for 120 min after 4',6-diamidino-2-phenylindole counterstaining at room temperature for 5 min. Images were captured with a fluorescence microscope system (DS-Ri2; Nikon Corporation). The Image-Pro Plus 6.0 image analysis software (Media Cybernetics, Inc.) was used for quantification analysis.

Determination of viability of CMECs. PA was dissolved in sodium hydroxide solution. Then, 10% BSA was added to the solution in order to form a PA and BSA complex. The solution was filter-sterilized, and then diluted with 1% BSA to prepare different concentrations of PA solutions, which were adjusted to pH 7.4. CMECs were seeded in 96-well plates (5,000 cells per well) and subjected to treatment with different concentrations (0, 100, 200, 400 and 800 μM) of PA with or without nicorandil (100 μM) at 37˚C for 24 h. Subsequently, 10 μl CCK-8 solution was added to the cell culture and the cells were incubated for 2 h at 37˚C in a humidifier (containing 5% CO_2 and 95% O_2). Finally, cell viability was determined at an optical density of 450 nm using a microplate reader.

Cell transfection. KLF2 overexpression and empty control pCMV plasmids were purchased from Shanghai GeneChem Co., Ltd. CMECs were seeded in 6-well plates ($1.0x10^5$ cells

per well) for 24 h prior to transfection. Cells were divided into the control group, control overexpression group and KLF2 overexpression group. Transient transfection was performed using Invitrogen Lipofectamine® 3000 (Thermo Fisher Scientific, Inc.) according to the standard protocol of the manufacturer. P3000 (Thermo Fisher Scientific, Inc.) combined with the overexpression-DNA (2.5 μg) or the control overexpression-DNA vectors (2.5 μg) was added to serum-free medium and incubated with the cells at 25˚C for 10 min, while the control group was treated without vectors. Subsequently, Lipofectamine 3000 was added to each group and cultured with the cells in serum-free ECM. Following 6 h of culture (37˚C; 5% CO_2), the medium was replaced with ECM containing 10% FBS. After 48 h, subsequent experiments were performed.

Small interfering RNAs targeting KLF2 (siKLF2) and the corresponding non-specific control (NC) siRNA were obtained from Sigma-Aldrich; Merck KGaA. Cells were divided into the control group, NC group and siKLF2 group. The control group was treated without siRNAs. The transfection procedures were performed according to the protocol described by Wang *et al* (35). siRNA (100 nM) was used for cell transfection using Lipofectamine® 3000 (Invitrogen; Thermo Fisher Scientific, Inc.). Cells were incubated at 37˚C with 5% CO_2. After a 6-h antibiotic-free medium incubation, the transfection medium was removed, and the cells were incubated in fresh medium for 24 h. Then, subsequent experiments were performed. All siRNA sequences are shown in Table SI. The transfection of KLF2 overexpression vector and siKLF2 was successful and KLF2 expression was increased and decreased, respectively (Fig. S2).

Statistical analysis. All experiments were performed at least three times, and all data are presented as the mean ± standard deviation. One-way analysis of variance was used to compare the differences among groups, and Tukey's post hoc test was used for multiple comparisons. All the statistical analyses were performed using IBM SPSS 25.0 software (IBM Corp.). $P<0.05$ (two-sided) was considered to indicate a statistically significant difference.

Results

Lipid infusion induces CMD. The CMD mouse model was successfully established by lipid infusion, which was characterized by a reduction of the CFR (model group vs. control group, 1.89±0.37 vs. 2.74±0.30; Fig. 1E). Serum tests revealed that the levels of FFAs in model mice were significantly increased, whereas the concentration of NO was decreased compared with those in control mice (Fig. 1B and C). Leukocyte activation in the cremaster microvascular wall was subsequently investigated (Fig. 1D). Lipid infusion led to a significantly increased level of leukocyte adhesion to the cremaster microvascular wall (model group vs. control group, 4,350±1,057.5 vs. 11.8±5.4 cells/mm^2) and a decreased leukocyte rolling velocity. However, the microvascular blood flow velocity, vascular diameter, leukocyte rolling flux and shear stress were found not to be impacted by lipid infusion.

To confirm whether lipid infusion caused structural changes in the mouse heart, the cardiac tissue was examined using H&E staining and TEM. No obvious structural changes were observed under the light microscope (Fig. 1F). However, TEM revealed severely swollen endothelial cells in the model group (Fig. 1G), demonstrating the damage of coronary microvascular ultrastructure.

To further investigate the effects of FFAs on CMECs, different concentrations of PA (0, 100, 200, 400 and 800 μM) were used to treat cultured CMECs *in vitro*, which revealed that 400 or 800 μM PA suppressed cell viability and increased ROS production in a dose-dependent manner (Fig. S3). Treatment with PA at a concentration of 400 μM for 24 h led to a reduction in cell viability of nearly 40% (Fig. S3A). Collectively, these results suggested that FFAs could induce CMD by damaging CMECs.

Nicorandil was found to alleviate CMD induced by lipid infusion, as demonstrated by an increase in the CFR and leukocyte rolling velocity, a decrease in the level of leukocyte adhesion and the improved endothelial damage (Fig. 1), the underlying mechanism of which was hypothesized to be associated with the upregulation of NO.

Lipid infusion induces an abnormal acute inflammatory response. Subsequently, the effects of lipid infusion on the inflammatory response were examined. Expression levels of the leukocyte adhesion molecule CD11b (Fig. 2A and B) and intracellular ROS levels (Fig. 2D) were found to be increased in the model mice, while the expression levels of CD62L on leukocytes were not altered (Fig. 2A and C). Subsequently, the levels of serum inflammatory markers were examined using ELISA. Higher serum levels of TNF-α and IL-6 were identified in the model group (Fig. 2F and G), whereas the serum SOD and IFN-γ levels were not significantly different between the model and control groups (Fig. 2E and H). Experiments using the AMPK activator, AICAR, also revealed anti-inflammatory effects with resultant reduced serum levels of TNF-α and IL-6 identified in AICAR-treated model mice (Fig. S4).

Lipid infusion inhibits the AMPK/KLF2/eNOS pathway. To assess the underlying mechanistic basis whereby FFAs could induce CMD, the AMPK/KLF2/eNOS pathway was subsequently analyzed via immunohistochemical and western blot analyses. Activation of AMPK and eNOS was assessed by detecting the levels of AMPK phosphorylation at Thr172 and eNOS phosphorylation at Ser117. As shown in Fig. 3A and B, lipid infusion led to downregulation of the expression level of KLF-2 and a decrease of the p-AMPK/AMPK and p-eNOS/eNOS ratios in the myocardium of model mice. Treatment of CMECs with 200, 400 and 800 μM PA *in vitro* caused significant suppression of the expression level of KLF2 and a decrease of the p-AMPK/AMPK and p-eNOS/eNOS ratios in a dose-dependent manner (Fig. 3C). Nicorandil increased the ratio of p-eNOS/eNOS and did not influence the expression of KLF2 or the ratio of p-AMPK/AMPK both *in vivo* (Fig. 3A and B) and *in vitro* (Fig. 3C). Nicorandil also improved CMEC viability and oxidative stress induced by PA (Fig. S5).

AMPK/KLF2/eNOS signaling pathway exerts an important role in regulating microvascular function. To further demonstrate that inhibition of the AMPK/KLF2/eNOS signaling pathway could account for CMD induced by FFAs, AICAR

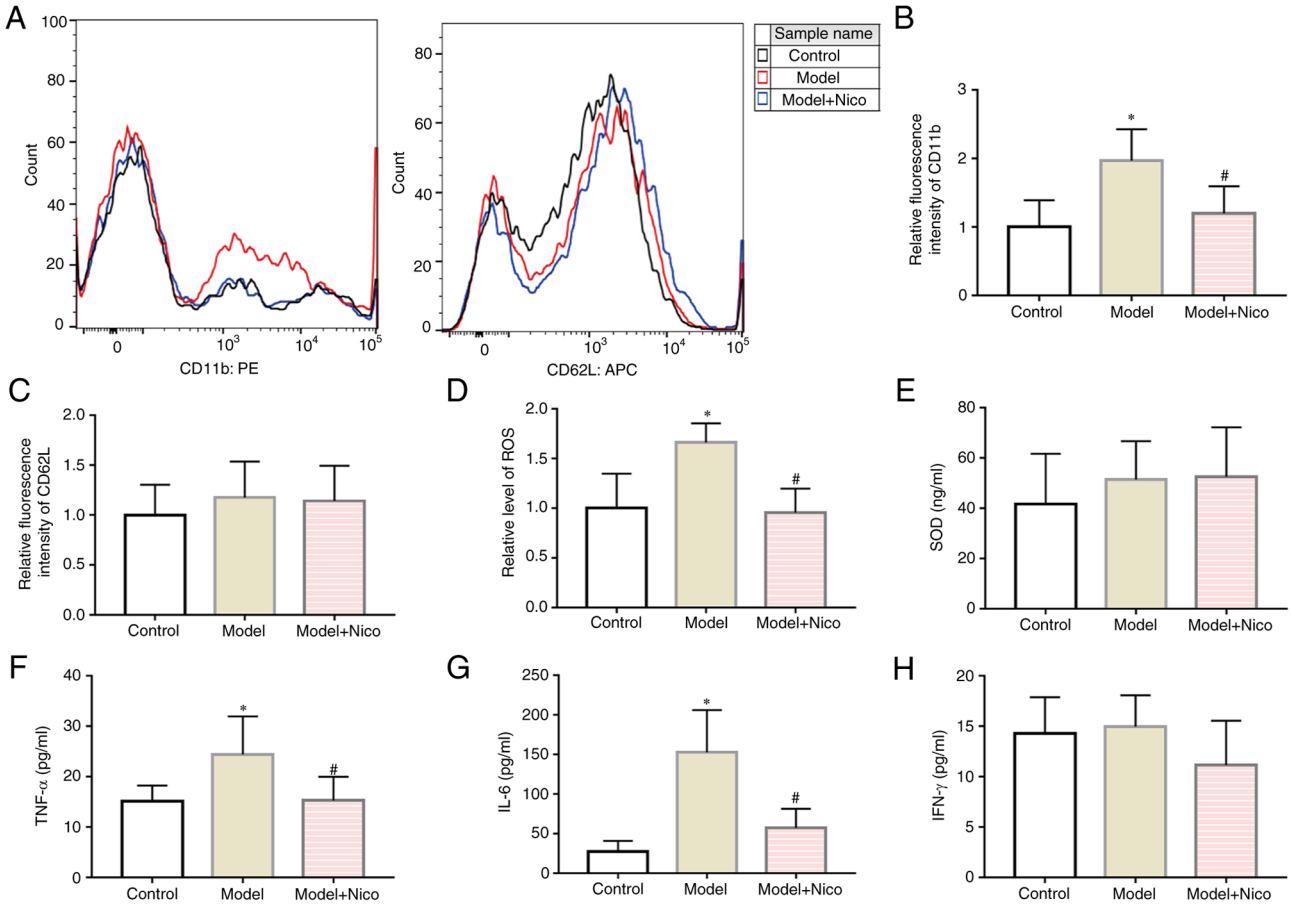

Figure 2. Lipid infusion upregulates CD11b expression in leukocytes, and exacerbates inflammation, whereas nicorandil treatment exerts anti-inflammatory effects. (A) Flow cytometric analysis of CD11b and CD62L. (B) CD11b expression on leukocytes relative to control group. (C) CD62L expression on leukocytes relative to control group. (D) Intracellular ROS levels of leukocytes relative to the control group. Serum (E) SOD, (F) TNF-α, (G) IL-6 and (H) IFN-γ levels. Data are presented as the mean ± SD. *P<0.05, Model (n=10) vs. Control (n=10); #P<0.05, Model + Nico (n=10) vs. Model (n=10). PE, phycoerythrin; APC, allophycocyanin; Nico, nicorandil; SOD, superoxide dismutase; ROS, reactive oxygen species.

was utilized to confirm whether activating AMPK could improve the condition of CMD in model mice. As shown in Fig. 4G and H, AICAR intervention *in vivo* did lead to an improvement in CFR and a decrease in leukocyte adhesion compared with those in model mice. *In vitro,* AICAR was found to enhance the viability of the CMECs and to inhibit oxidative stress (Fig. 4B and C). AICAR also led to an increase in the expression of both AMPK and the downstream proteins, KLF2 and eNOS, in CMECs (Fig. 4A). Subsequently, KLF2 overexpression plasmid was used to evaluate the effect of KLF2 on the phosphorylation of eNOS. As shown in Fig. S2A, KLF2 was found to be overexpressed. KLF2 overexpression, in itself, led to significant upregulation of eNOS in CMECs treated with PA, although it exerted no significant effects on AMPK (Fig. 4D). Either upregulation of KLF2 with the overexpression plasmid or increasing the concentration of NO with nicorandil led to both an improvement in the viability of CMECs and inhibition of oxidative stress (Figs. 4E and F, and S5). However, when siKLF2 was used to suppress KLF2 expression in CMECs, AICAR did increase the ratio of p-AMPK/AMPK but did not increase the expression of KLF2 or the ratio of p-eNOS/eNOS (Fig. S6). Taken together, the underlying mechanism through which FFAs induce CMD may involve disruption of the AMPK/KLF2/eNOS signaling pathway.

Discussion

A high level of FFAs is a risk factor for cardiovascular disease due to their detrimental effects on vascular endothelial cells, which is common in patients with myocardial ischemia (36). This may be due to the increased sympathetic drive under myocardial ischemia promoting the release of FFAs into the blood through the activation of lipolysis in adipose tissue (37). However, elevation of the level of FFAs in myocardial ischemia has been demonstrated to increase ischemic damage of the myocardium (38). Availability of FFAs in the circulation reciprocally reduces cardiac glucose utilization, whereas oxidation of fatty acids requires more oxygen per adenosine triphosphate produced than glucose (39). Therefore, increased cardiac utilization of fatty acids will lead to increased oxygen consumption and make the heart more susceptible to ischemic events (40).

An acute increase in the serum FFA level triggers inflammation and oxidative stress in the endothelium (41). Ko *et al* (42) reported that FFAs, as nutrient stress factors, could activate cardiac inflammation and suppress myocardial glucose metabolism via inhibition of AMPK in the heart. Han *et al* (43) also revealed that FFAs could induce cardiac dysfunction and alter insulin-signaling pathways. High serum concentrations of FFAs can lead to both microvascular and

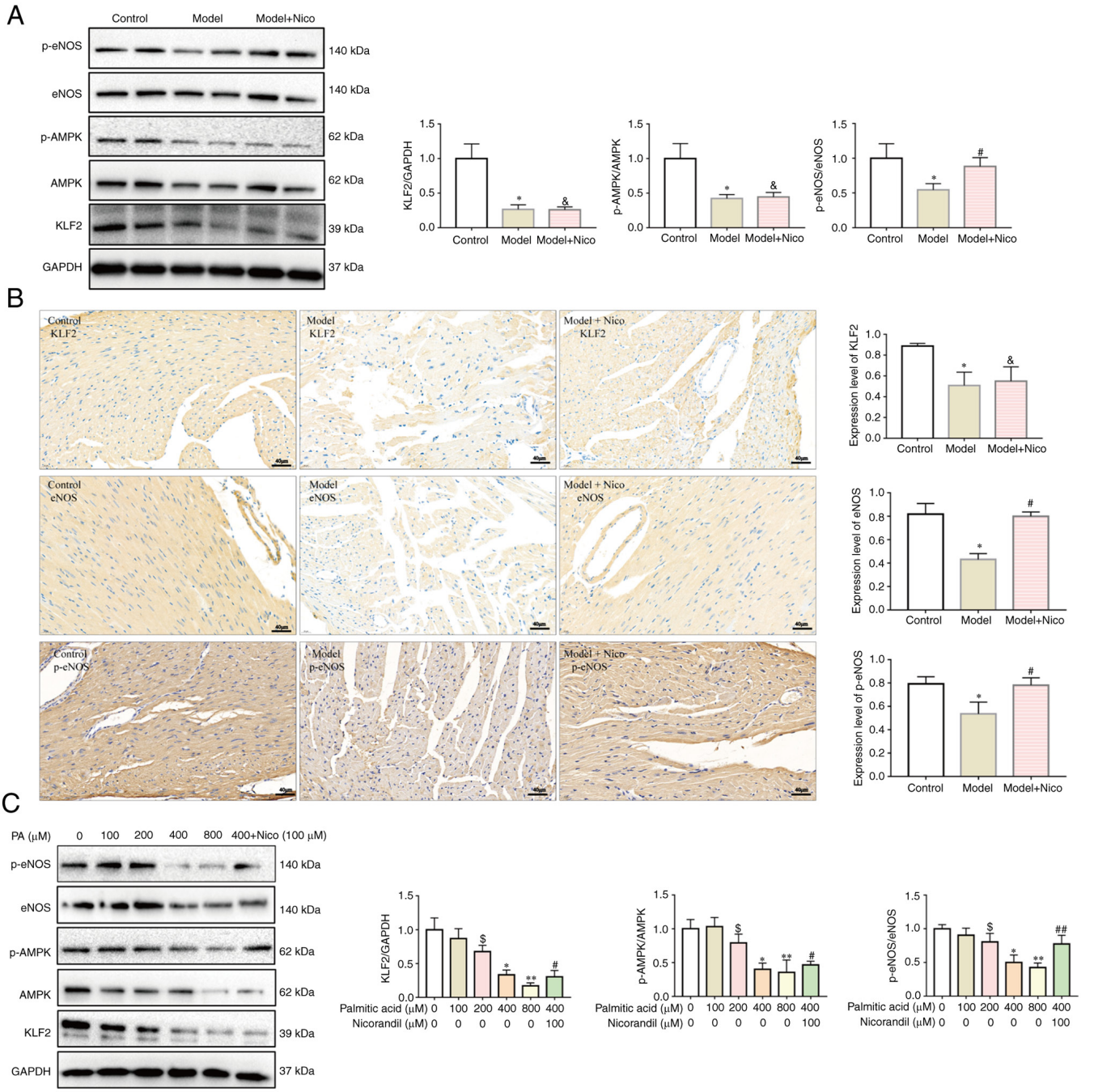

Figure 3. Lipid infusion inhibits the AMPK/KLF2/eNOS signaling pathway, whereas nicorandil treatment upregulates eNOS expression. (A) Expression levels of KLF2, p-AMPK/AMPK and p-eNOS/eNOS were decreased in the heart tissues of model mice, as assessed by western blotting. Data are presented as the mean ± SD. *P<0.05, Model (n=6) vs. Control (n=6). $^{\#}$P<0.05, Model + Nico (n=6) vs. Model (n=6). $^{\&}$P<0.05, Model + Nico (n=6) vs. Control (n=6). (B) Expression levels of KLF2, eNOS and p-eNOS were decreased in heart tissues of model mice, as assessed by immunohistochemistry. Scale bar, 40 μm. Data are presented as the mean ± SD. *P<0.05, Model (n=5) vs. Control (n=5). $^{\#}$P<0.05, Model + Nico (n=5) vs. Model (n=5). $^{\&}$P<0.05, Model + Nico (n=5) vs. Control (n=5). (C) Expression levels of KLF2, and ratios of p-AMPK/AMPK and p-eNOS/eNOS were decreased in cardiac microvascular endothelial cells treated with PA in a dose-dependent manner, as assessed by western blotting. Data are presented as the mean ± SD. $^{\$}$P<0.05, PA, 200 μM (n=6) vs. PA, 0 μM (n=6). *P<0.05, PA, 400 μM (n=6) vs. PA, 0 μM (n=6). **P<0.05, PA, 800 μM (n=6) vs. PA, 0 μM (n=6). $^{\#}$P<0.05, PA, 400 μM + Nicorandil, 100 μM (n=6) vs. PA, 0 μM (n=6). $^{\#\#}$P<0.05, PA, 400 μM + Nicorandil, 100 μM (n=6) vs. PA, 400 μM (n=6). AMPK, AMP-activated protein kinase; eNOS, endothelial nitric oxide synthase; KLF2, Krüppel-like factor 2; Nico, nicorandil; p-, phosphorylated; PA, palmitic acid.

metabolic insulin resistance (44). Endothelial dysfunction is a major mechanism associated with CMD (2) and, based on these findings, our hypothesis was that abnormal FFA metabolism may serve an important role in the pathogenesis of CMD by influencing endothelial function.

A common approach for experimentally elevating plasma FFA levels is to simultaneously infuse heparin and a lipid emulsion (45-47), as was accomplished in our previous study (16), and in the present study. Heparin can activate lipoprotein lipase and catalyzes triglyceride hydrolysis, which increases the serum concentration of FFAs (48). The elevation of FFAs achieved by the infusion of heparin and lipids leads to rapid induction of endothelial dysfunction (49,50). To further understand the deleterious effects of FFAs on CMD, a mouse model of systemic

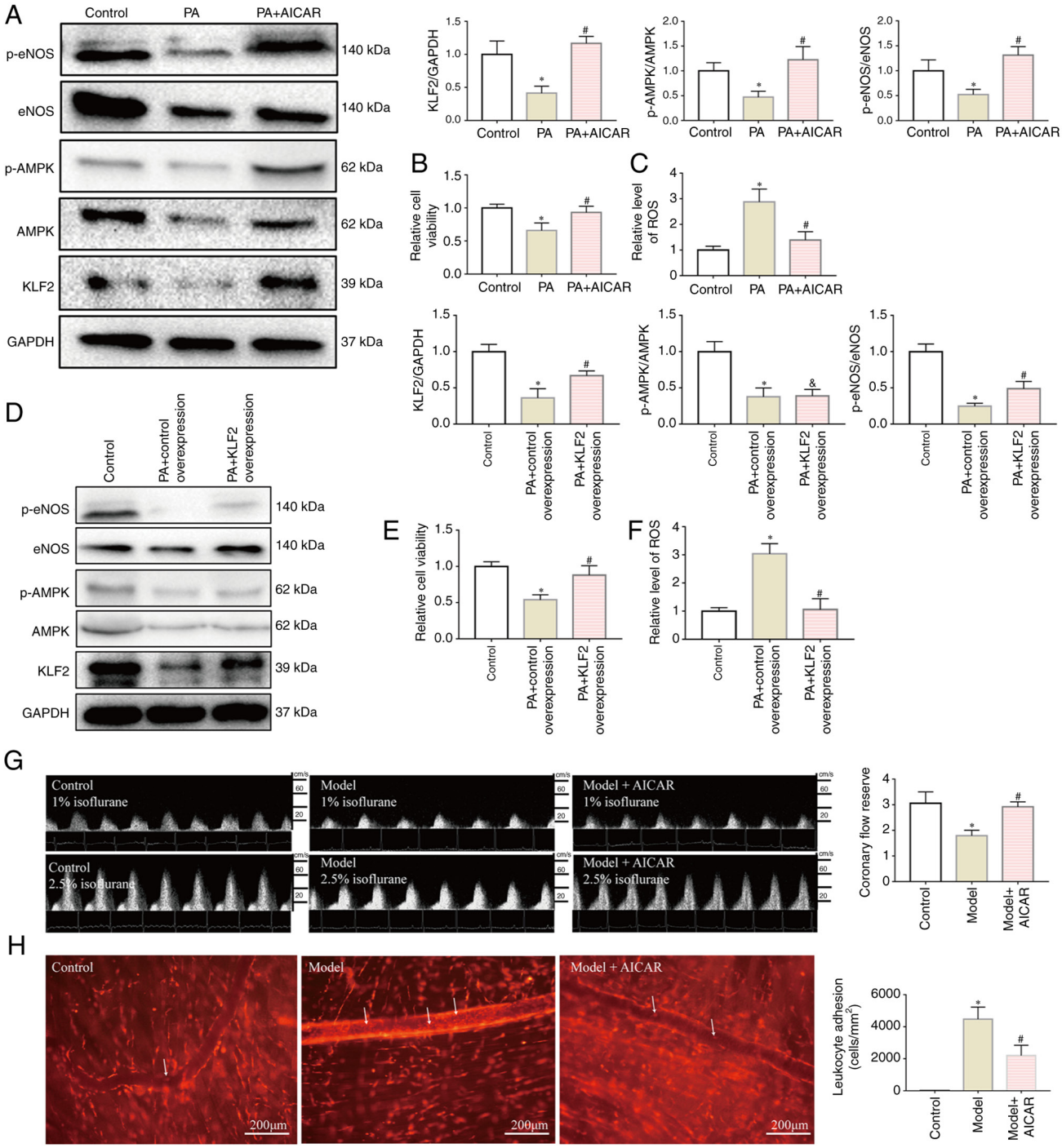

Figure 4. AMPK/KLF2/eNOS pathway serves an important role in regulating microvascular function. (A) AICAR activated the AMPK/KLF2/eNOS pathway in CMECs. AICAR treatment upregulated the levels of KLF2, p-AMPK/AMPK and p-eNOS/eNOS. Data are presented as the mean ± SD. *P<0.05, PA (n=6) vs. Control (n=6). #P<0.05; PA + AICAR (n=6) vs. PA (n=6). (B and C) AICAR restored the viability of CMECs and caused a decrease in the levels of intracellular ROS. (B) Cell viability relative to the control group. (C) ROS level relative to the control group. Data are presented as the mean ± SD. *P<0.05, PA (n=6) vs. Control (n=6); #P<0.05, PA + AICAR (n=6) vs. PA (n=6). (D) KLF2 overexpression activated eNOS in CMECs and did not influence the expression of AMPK. Data are presented as the mean ± SD. *P<0.05, PA + Control Overexpression (n=6) vs. Control (n=6); #P<0.05, PA + KLF2 Overexpression (n=6) vs. PA + Control Overexpression (n=6); &P<0.05, PA + KLF2 Overexpression (n=6) vs. Control (n=6). (E and F) KLF2 overexpression restored the viability of the CMECs and led to a decrease in intracellular ROS. (E) Cell viability relative to the control group. (F) ROS level relative to the control group. Data are presented as the mean ± SD. *P<0.05, PA + Control Overexpression (n=6) vs. Control (n=6); #P<0.05, PA + KLF2 Overexpression (n=6) vs. PA + Control Overexpression (n=6). (G) AICAR treatment increased the coronary flow reserve of model mice. (H) AICAR treatment decreased the levels of leukocyte adhesion (white arrows indicate the leukocytes that adhered to the cremaster microvascular wall). Data are presented as the mean ± SD. *P<0.05, Model (n=5) vs. Control (n=5); #P<0.05, Model + AICAR (n=5) vs. Model (n=5). Scale bar, 200 μm. AICAR, 5-aminoimidazole-4-carboxamide ribonucleotide; AMPK, AMP-activated protein kinase; CMD, coronary microvascular dysfunction; CMECs, cardiac microvascular endothelial cells; eNOS, endothelial nitric oxide synthase; KLF2, Krüppel-like factor 2; p-, phosphorylated; PA, palmitic acid; ROS, reactive oxygen species.

microvascular dysfunction was established via infusion of lipid emulsion with heparin to increase the concentration of serum FFAs. After lipid emulsion infusion, the serum concentration of FFAs was found to increase to more than twice the normal value.

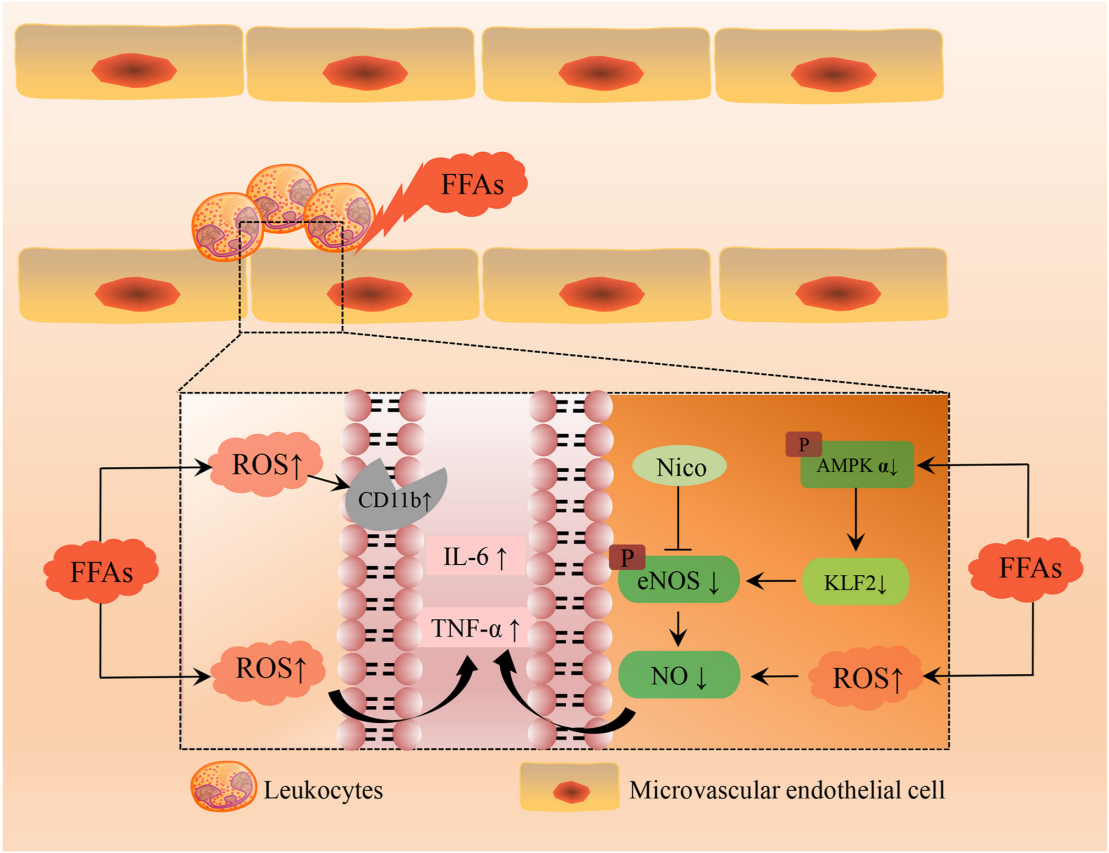

Figure 5. Potential mechanisms of FFA-induced coronary microvascular dysfunction. AMPK, AMP-activated protein kinase; eNOS, endothelial nitric oxide synthase; FFA, free fatty acid; KLF2, Krüppel-like factor 2; Nico, nicorandil; NO, nitric oxide; ROS, reactive oxygen species; p, phosphorylated.

In the present study, the model group exhibited a reduction in CFR of >30%, indicating that CMD had been established. A large number of leukocytes were found to adhere to the walls of microvessels, indicating that leukocyte activation and the impairment of microvascular endothelial function had occurred. In addition, the use of TEM revealed the presence of swelling of microvascular endothelial cells in the heart tissues and palmitic acid were demonstrated to cause a decrease in the viability of CMECs in a dose-dependent manner. Both phenomena indicated the damage to CMECs that had been caused by FFAs. Endothelial dysfunction and leukocyte activation may be the key processes of CMD induced by FFAs. Following intravenous infusion of the lipid emulsion, the production of ROS in the model group was found to be increased. In the present study, high levels of FFAs were able to stimulate the production of ROS in both leukocytes and CMECs. Excessive ROS production leads to the oxidative damage of numerous biological macromolecules, including nucleic acids, lipids, proteins and carbohydrates, which subsequently affects multiple physiological metabolic pathways (51). Postprandial hyperlipidemia has been reported to be associated with acute endothelial dysfunction (52). In the present study, it was also found that CD11b expression was markedly increased in the model group. CD11b is directly involved in cell adhesion and leukocyte activation (53). Endothelial cell adhesion molecules bind to leukocytes, thereby activating them and leading to their infiltration into the underlying tissues (54). Activated leukocytes not only block microvessels, but also cause an increase in the vascular permeability (55). Compared with those in control mice, the levels of the plasma pro-inflammatory factors, IL-6 and TNF-α, were found to be significantly increased following lipid emulsion infusion. An increase in the level of IL-6 is able to initiate the acute inflammatory reaction, and inhibition of IL-6 has previously been reported to reduce the risk of atherosclerotic thrombotic events (56). As far as TNF-α is concerned, an increase in its level has been demonstrated to induce endothelial cells to express adhesion factors, accelerate the adhesion and penetration of leukocytes into the vascular endothelium, and cause local inflammatory reactions and pannus formation (57). Microvascular endothelial dysfunction and abnormal activation of leukocytes are processes that interact with and mutually enhance each other (58), thereby fulfilling an important role in the pathophysiological mechanism of FFA-induced CMD.

Extensive studies have demonstrated that AMPK is activated by an energy deficiency but suppressed by overnutrition (59,60). In the present study, the increased serum concentration of FFAs led to a significant inhibition of the activation of AMPK. Dysregulation of the AMPK/KLF2/eNOS signaling pathway may be responsible for the mechanism that accounts for the induction of CMD mediated by FFAs (Fig. 5). On one side, elevated FFAs can activate leukocytes and increase ROS, promoting the production of CD11b, IL-6 and TNF-α. On the other side, FFAs caused NO reduction in CMECs by blocking the AMPK/KLF2/eNOS pathway. This resulted in decreased cell viability and impaired endothelial

function, which eventually induces the development of CMD. In the model group, the expression levels of AMPK, KLF2 and eNOS in myocardial tissue were downregulated, and the serum NO level was decreased. *In vitro* experiments subsequently demonstrated that treatment with PA caused a decrease in the expression levels of AMPK, KLF2 and eNOS in a dose-dependent manner. These results suggested that FFAs may suppress the AMPK/KLF2 signaling pathway in CMECs, thereby inhibiting endothelial function and reducing NO production. Increased serum levels of FFAs can cause endoplasmic reticulum stress and mitochondrial dysfunction, which lead to a disordering of energy metabolism and biosynthesis (13). It is well established that the AMPK signaling pathway is closely associated with energy metabolism (18). Wang *et al* (61) found that PA reduced AMPK phosphorylation, and activation of the AMPK signaling pathway could improve mitochondrial function by inhibiting lipid aggregation. KLF2 is an important regulator of endothelial function, which is able to activate eNOS (24). Decreased KLF2 expression levels are associated with endothelial dysfunction induced by advanced glycation end products (62). KLF2 is widely regarded as the most potent inducer of eNOS, especially under laminar shear stress (63). Furthermore, the AMPK/KLF2 signaling pathway has been demonstrated to participate in neovascular development following cerebral ischemia via the regulation of eNOS protein expression (25). In order to further verify that the decreased AMPK activity was associated with the downstream proteins KLF2 and eNOS, the AMPK activator AICAR was used to treat the CMECs and these experiments revealed that activation of AMPK could significantly improve PA-induced inhibition of KLF2 and eNOS. AICAR is an AMPK agonist, which can promote AMPK phosphorylation (64). Viglino *et al* (65) reported that chronic treatment with AICAR induces a metabolic shift in FFA-exposed cardiomyocytes, characterized by improved glucose transport and glycolysis and redirection of fatty acids towards neutral storage. Hu *et al* (66) found that AICAR treatment led to an improvement in liver fibrosis in rats with bile duct ligation by increasing the level of NO. Acute and chronic use of AICAR have been demonstrated to relieve portal vein pressure without changing systemic hemodynamics (66). AICAR can also alleviate endothelial dysfunction and promote vasodilation by improving eNOS activity and increasing NO production (67,68). The present study also demonstrated that an injection of AICAR relieved FFA-induced CMD and enhanced CFR. In addition, a KLF2 overexpression plasmid was transfected into CMECs, and KLF2 overexpression was found to activate eNOS. However, when combing AICAR and siKLF2 to treat CMECs, KLF2 or eNOS expression was not increased. Therefore, the aforementioned results further suggested that FFAs may serve a role in coronary microcirculation damage by interfering with the AMPK/KLF2/eNOS signaling pathway.

Nicorandil is commonly used to relieve the microvascular angina that is called cardiac syndrome X (69). A recent meta-analysis of randomized controlled trials confirmed that nicorandil has potential in terms of improving angina symptoms in cardiac syndrome X (69). Nicorandil is also one of the few drugs available that have been evidentially demonstrated to effectively treat CMD (70). The present study demonstrated that nicorandil could increase the CFR and reduce the level of leukocyte adhesion in FFA-induced CMD model mice. Nicorandil also alleviated swelling of the microvascular endothelium caused by FFAs, increased the viability of CMECs, and caused a reduction in ROS production. Increased production of NO was likely to account for the effects of nicorandil. Nicorandil can not only function as a NO donor, but also modulate eNOS (71,72). The present study demonstrated that nicorandil could directly activate eNOS without the participation of AMPK. In addition, nicorandil fulfilled an anti-inflammatory role, leading to reduced levels of IL-6 and TNF-α in the plasma. A clinical trial has suggested that nicorandil treatment may result in cardiovascular protection by inhibiting systemic inflammation (73). In the present study, nicorandil could stimulate eNOS expression and facilitate NO production in CMECs. Nicorandil also exerted anti-inflammatory and antioxidant effects. Previous studies have concluded that nicorandil could attenuate organ injury by increasing eNOS expression and via its antiapoptotic, anti-inflammatory and antioxidant properties (71,74).

Reducing chronic serum FFA levels may reduce the cardiovascular disease burden, and thus, efforts have been made to develop pharmaceuticals to reduce the level of serum FFAs (75). Oral phytosterol supplementation has been demonstrated to cause a reduction in serum FFAs (76). Lifestyle interventions are also useful; for example, a previous meta-analysis of randomized controlled trials revealed a reduction of FFAs with chronic exercise training (77). Research in this field is ongoing, although, at present, it has not yet yielded any approved drugs aimed at suppressing the serum FFA concentration (78).

The present study still has several limitations to be disclosed. Firstly, there are endothelia-dependent and endothelia-independent mechanisms operative in the pathogenesis of CMD (4). In the present study, only the effects on endothelial factors were explored and further research is required in this regard. Secondly, pan-endothelial cell markers were not tested by immunohistochemistry analysis. Thirdly, the long-term efficacy of nicorandil remains to be validated.

In conclusion, the present study demonstrated that FFAs could induce CMD via inhibition of the AMPK/KLF2/eNOS signaling pathway, whereas activation of this pathway alleviated FFA-induced CMD, which could be a therapeutic option for CMD.

Acknowledgements

Not applicable.

Funding

This work was supported by the National Natural Science Foundation of China (grant nos. 82120108004 and 82104588), the Shanghai Science and Technology Innovation Action Plan (grant no. 22DZ2304500), and the Pyramid Talent Program of Changzheng Hospital (grant no. YQ662).

Availability of data and materials

The datasets used and/or analyzed during the current study are available from the corresponding author on reasonable request.

Authors' contributions

YZ, JZ, ZH and CL designed the experiments. YZ, JZ, CR and BH performed the experiments. YZ, JZ and RD analyzed the data. YZ, JZ, ZH and CL wrote and revised the manuscript. JZ and CL acquired the funding. YZ and CL confirmed the authenticity of all the raw data. All authors have read and approved the final manuscript.

Ethics approval and consent to participate

The entire animal experimental protocol used in the present study was carefully checked and approved by the Animal Experiment Ethics Committee of the Second Affiliated Hospital of Naval Medical University (no. 2020SL037; Shanghai, China). All animal care procedures were carried out in accordance with the Animal Research: Reporting of *In Vivo* Experiments guidelines on animal research.

Patient consent for publication

Not applicable.

Competing interests

The authors declare that they have no competing interests.

References

1. GBD 2015 Mortality and Causes of Death Collaborators: Global, regional, and national life expectancy, all-cause mortality, and cause-specific mortality for 249 causes of death, 1980-2015: A systematic analysis for the global burden of disease study 2015. Lancet 388: 1459-1544, 2016.
2. Vancheri F, Longo G, Vancheri S and Henein M: Coronary microvascular dysfunction. J Clin Med 9: 2880, 2020.
3. Murthy VL, Naya M, Taqueti VR, Foster CR, Gaber M, Hainer J, Dorbala S, Blankstein R, Rimoldi O, Camici PG and Di Carli MF: Effects of sex on coronary microvascular dysfunction and cardiac outcomes. Circulation 129: 2518-2527, 2014.
4. Del BM, Montone RA, Camilli M, Carbone S, Narula J, Lavie CJ, Niccoli G and Crea F: Coronary microvascular dysfunction across the spectrum of cardiovascular diseases: JACC state-of-the-art review. J Am Coll Cardiol 78: 1352-1371, 2021.
5. Thakker RA, Rodriguez Lozano J, Rodriguez Lozano P, Motiwala A, Rangasetty U, Khalife W and Chatila K: Coronary microvascular disease. Cardiol Ther 11: 23-31, 2022.
6. Niu Z, Hu H and Tang F: High free fatty acid levels are associated with stroke recurrence and poor functional outcome in Chinese patients with ischemic stroke. J Nutr Health Aging 21: 1102-1106, 2017.
7. Jung Y, Cho Y, Kim N, Oh IY, Kang SW, Choi EK and Hwang GS: Lipidomic profiling reveals free fatty acid alterations in plasma from patients with atrial fibrillation. PLoS One 13: e196709, 2018.
8. Skidmore PML, Woodside JV, Mc Master C, Bingham A, Mercer C, Evans A, Young IS and Yarnell JW: Plasma free fatty acid patterns and their relationship with CVD risk in a male middle-aged population. Eur J Clin Nutr 64: 239-244, 2010.
9. Khawaja O, Maziarz M, Biggs ML, Longstreth WT Jr, Ix JH, Kizer JR, Zieman S, Tracy RP, Mozaffarian D, Mukamal KJ, *et al*: Plasma free fatty acids and risk of stroke in the cardiovascular health study. Int J Stroke 9: 917-920, 2014.
10. Pilz S and März W: Free fatty acids as a cardiovascular risk factor. Clin Chem Lab Med 46: 429-434, 2008.
11. Hu T, Zhang W, Han F, Zhao R, Liu L and An Z: Plasma fingerprint of free fatty acids and their correlations with the traditional cardiac biomarkers in patients with type 2 diabetes complicated by coronary heart disease. Front Cardiovasc Med 9: 903412, 2022.
12. Lopaschuk GD, Ussher JR, Folmes CD, Jaswal JS and Stanley WC: Myocardial fatty acid metabolism in health and disease. Physiol Rev 90: 207-258, 2010.
13. Fillmore N, Mori J and Lopaschuk GD: Mitochondrial fatty acid oxidation alterations in heart failure, ischaemic heart disease and diabetic cardiomyopathy. Br J Pharmacol 171: 2080-2090, 2014.
14. Goldberg IJ, Trent CM and Schulze PC: Lipid metabolism and toxicity in the heart. Cell Metab 15: 805-812, 2012.
15. Wende AR and Abel ED: Lipotoxicity in the heart. Biochim Biophys Acta 1801: 311-319, 2010.
16. Zhang Y, Zhao J, Ding R, Niu W, He Z and Liang C: Pre-treatment with compound Danshen dripping pills prevents lipid infusion-induced microvascular dysfunction in mice. Pharm Biol 58: 701-706, 2020.
17. Niu Y, Li S, Na L, Feng R, Liu L, Li Y and Sun C: Mangiferin decreases plasma free fatty acids through promoting its catabolism in liver by activation of AMPK. PLoS One 7: e30782, 2012.
18. Qi D and Young LH: AMPK: Energy sensor and survival mechanism in the ischemic heart. Trends Endocrinol Metab 26: 422-429, 2015.
19. Baltgalvis KA, White K, Li W, Claypool MD, Lang W, Alcantara R, Singh BK, Friera AM, McLaughlin J, Hansen D, *et al*: Exercise performance and peripheral vascular insufficiency improve with AMPK activation in high-fat diet-fed mice. Am J Physiol Heart Circ Physiol 306: H1128-H1145, 2014.
20. Atkins GB and Jain MK: Role of Krüppel-like transcription factors in endothelial biology. Circ Res 100: 1686-1695, 2007.
21. Chatauret N, Coudroy R, Delpech PO, Vandebrouck C, Hosni S, Scepi M and Hauet T: Mechanistic analysis of nonoxygenated hypothermic machine perfusion's protection on warm ischemic kidney uncovers greater eNOS phosphorylation and vasodilation. Am J Transplant 14: 2500-2514, 2014.
22. Hong FF, Liang XY, Liu W, Lv S, He SJ, Kuang HB and Yang SL: Roles of eNOS in atherosclerosis treatment. Inflamm Res 68: 429-441, 2019.
23. Yan J, Wang A, Cao J and Chen L: Apelin/APJ system: An emerging therapeutic target for respiratory diseases. Cell Mol Life Sci 77: 2919-2930, 2020.
24. Lee GH, Park JS, Jin SW, Pham TH, Thai TN, Kim JY, Kim CY, Choi JH, Han EH and Jeong HG: Betulinic acid induces eNOS expression via the AMPK-dependent KLF2 signaling pathway. J Agric Food Chem 68: 14523-14530, 2020.
25. Chen GH, Li XL, Deng YQ, Zhou FM, Zou WQ, Jiang WX, Shangguan SQ and Lu ZN: The molecular mechanism of EPO regulates the angiogenesis after cerebral ischemia through AMPK-KLF2 signaling pathway. Crit Rev Eukaryot Gene Expr 29: 105-112, 2019.
26. Segers VFM, Brutsaert DL and De Keulenaer GW: Cardiac remodeling: endothelial cells have more to say than just NO. Front Physiol 9: 382, 2018.
27. Jiang P, Ren L, Zhi L, Yu Z, Lv F, Xu F, Peng W, Bai X, Cheng K, Quan L, *et al*: Negative regulation of AMPK signaling by high glucose via E3 ubiquitin ligase MG53. Mol Cell 81: 629-637.e5, 2021.
28. Percie du Sert N, Hurst V, Ahluwalia A, Alam S, Avey MT, Baker M, Browne WJ, Clark A, Cuthill IC, Dirnagl U, *et al*: The ARRIVE guidelines 2.0: Updated guidelines for reporting animal research. Br J Pharmacol 177: 3617-3624, 2020.
29. Zhan B, Xu Z, Zhang Y, Wan K, Deng H, Wang D, Bao H, Wu Q, Hu X, Wang H, *et al*: Nicorandil reversed homocysteine-induced coronary microvascular dysfunction via regulating PI3K/Akt/eNOS pathway. Biomed Pharmacother 127: 110121, 2020.
30. Chang WT, Fisch S, Chen M, Qiu Y, Cheng S and Liao R: Ultrasound based assessment of coronary artery flow and coronary flow reserve using the pressure overload model in mice. J Vis Exp: e52598, 2015.
31. Wang Y, Du F, Hawez A, Mörgelin M and Thorlacius H: Neutrophil extracellular trap-microparticle complexes trigger neutrophil recruitment via high-mobility group protein 1 (HMGB1)-toll-like receptors (TLR2)/TLR4 signalling. Br J Pharmacol 176: 3350-3363, 2019.
32. House SD and Lipowsky HH: Leukocyte-endothelium adhesion: Microhemodynamics in mesentery of the cat. Microvasc Res 34: 363-379, 1987.
33. McDonald CA, Payne NL, Sun G, Moussa L, Siatskas C, Lim R, Wallace EM, Jenkin G and Bernard CC: Immunosuppressive potential of human amnion epithelial cells in the treatment of experimental autoimmune encephalomyelitis. J Neuroinflammation 12: 112, 2015.

34. Johnson EK, Schelling ME, Quitadamo IJ, Andrew S and Johnson EC: Cultivation and characterization of coronary microvascular endothelial cells: A novel porcine model using micropigs. Microvasc Res 64: 278-288, 2002.
35. Wang C, He H, Liu G, Ma H, Li L, Jiang M, Lu Q, Li P and Qi H: DT-13 induced apoptosis and promoted differentiation of acute myeloid leukemia cells by activating AMPK-KLF2 pathway. Pharmacol Res 158: 104864, 2020.
36. Roy VK, Kumar A, Joshi P, Arora J and Ahanger AM: Plasma free fatty acid concentrations as a marker for acute myocardial infarction. J Clin Diagn Res 7: 2432-2434, 2013.
37. Hendrickson SC, St Louis JD, Lowe JE and Abdel-aleem S: Free fatty acid metabolism during myocardial ischemia and reperfusion. Mol Cell Biochem 166: 85-94, 1997.
38. Manzella D, Barbieri M, Rizzo MR, Ragno E, Passariello N, Gambardella A, Marfella R, Giugliano D and Paolisso G: Role of free fatty acids on cardiac autonomic nervous system in noninsulin-dependent diabetic patients: Effects of metabolic control. J Clin Endocrinol Metab 86: 2769-2774, 2001.
39. Knuuti MJ, Mäki M, Yki-Järvinen H, Voipio-Pulkki LM, Härkönen R, Haaparanta M and Nuutila P: The effect of insulin and FFA on myocardial glucose uptake. J Mol Cell Cardiol 27: 1359-1367, 1995.
40. Lopaschuk GD: Metabolic modulators in heart disease: Past, present, and future. Can J Cardiol 33: 838-849, 2017.
41. I S Sobczak A, A Blindauer C and J Stewart A: Changes in plasma free fatty acids associated with type-2 diabetes. Nutrients 11: 2022, 2019.
42. Ko HJ, Zhang Z, Jung DY, Jun JY, Ma Z, Jones KE, Chan SY and Kim JK: Nutrient stress activates inflammation and reduces glucose metabolism by suppressing AMP-activated protein kinase in the heart. Diabetes 58: 2536-2546, 2009.
43. Han L, Liu J, Zhu L, Tan F, Qin Y, Huang H and Yu Y: Free fatty acid can induce cardiac dysfunction and alter insulin signaling pathways in the heart. Lipids Health Dis 17: 185, 2018.
44. Chai W, Liu J, Jahn LA, Fowler DE, Barrett EJ and Liu Z: Salsalate attenuates free fatty acid-induced microvascular and metabolic insulin resistance in humans. Diabetes Care 34: 1634-1638, 2011.
45. Tripathy D, Mohanty P, Dhindsa S, Syed T, Ghanim H, Aljada A and Dandona P: Elevation of free fatty acids induces inflammation and impairs vascular reactivity in healthy subjects. Diabetes 52: 2882-2887, 2003.
46. Turpin SM, Ryall JG, Southgate R, Darby I, Hevener AL, Febbraio MA, Kemp BE, Lynch GS and Watt MJ: Examination of 'lipotoxicity' in skeletal muscle of high-fat fed and ob/ob mice. J Physiol 587: 1593-1605, 2009.
47. Boden G, She P, Mozzoli M, Cheung P, Gumireddy K, Reddy P, Xiang X, Luo Z and Ruderman N: Free fatty acids produce insulin resistance and activate the proinflammatory nuclear factor-kappaB pathway in rat liver. Diabetes 54: 3458-3465, 2005.
48. Yasu T, Mutoh A, Wada H, Kobayashi M, Kikuchi Y, Momomura S and Ueda S: Renin-angiotensin system inhibitors can prevent intravenous lipid infusion-induced myocardial microvascular dysfunction and leukocyte activation. Circ J 82: 494-501, 2018.
49. Umpierrez GE, Smiley D, Robalino G, Peng L, Kitabchi AE, Khan B, Le A, Quyyumi A, Brown V and Phillips LS: Intravenous intralipid-induced blood pressure elevation and endothelial dysfunction in obese African-Americans with type 2 diabetes. J Clin Endocrinol Metab 94: 609-614, 2009.
50. Wang H, Li H, Hou Z, Pan L, Shen X and Li G: Role of oxidative stress in elevated blood pressure induced by high free fatty acids. Hypertens Res 32: 152-158, 2009.
51. Guerra BA and Otton R: Impact of the carotenoid astaxanthin on phagocytic capacity and ROS/RNS production of human neutrophils treated with free fatty acids and high glucose. Int Immunopharmacol 11: 2220-2226, 2011.
52. Mah E, Noh SK, Ballard KD, Matos ME, Volek JS and Bruno RS: Postprandial hyperglycemia impairs vascular endothelial function in healthy men by inducing lipid peroxidation and increasing asymmetric dimethylarginine:arginine. J Nutr 141: 1961-1968, 2011.
53. Dong G, Song L, Tian C, Wang Y, Miao F, Zheng J, Lu C, Alsadun S and Graves DT: FOXO1 regulates bacteria-induced neutrophil activity. Front Immunol 8: 1088, 2017.
54. Gomes NE, Brunialti MK, Mendes ME, Freudenberg M, Galanos C and Salomão R: Lipopolysaccharide-induced expression of cell surface receptors and cell activation of neutrophils and monocytes in whole human blood. Braz J Med Biol Res 43: 853-858, 2010.
55. Zhang H, Wang Y, Qu M, Li W, Wu D, Cata JP and Miao C: Neutrophil, neutrophil extracellular traps and endothelial cell dysfunction in sepsis. Clin Transl Med 13: e1170, 2023.
56. Ridker PM, Libby P, MacFadyen JG, Thuren T, Ballantyne C, Fonseca F, Koenig W, Shimokawa H, Everett BM and Glynn RJ: Modulation of the interleukin-6 signalling pathway and incidence rates of atherosclerotic events and all-cause mortality: Analyses from the canakinumab anti-inflammatory thrombosis outcomes study (CANTOS). Eur Heart J 39: 3499-3507, 2018.
57. Jiang T, Zhang W and Wang Z: Laquinimod protects Against TNF-α-induced attachment of monocytes to human aortic endothelial cells (HAECs) by increasing the expression of KLF2. Drug Des Devel Ther 14: 1683-1691, 2020.
58. Wang Y, Zhang J, Wang Z, Wang C and Ma D: Endothelial-cell-mediated mechanism of coronary microvascular dysfunction leading to heart failure with preserved ejection fraction. Heart Fail Rev 28: 169-178, 2023.
59. Hardie DG and Carling D: The AMP-activated protein kinase-fuel gauge of the mammalian cell? Eur J Biochem 246: 259-273, 1997.
60. Coughlan KA, Valentine RJ, Ruderman NB and Saha AK: Nutrient excess in AMPK downregulation and insulin resistance. J Endocrinol Diabetes Obes 1: 1008, 2013.
61. Wang Q, Wang Z, Xu M, Tu W, Hsin IF, Stotland A, Kim JH, Liu P, Naiki M, Gottlieb RA and Seki E: Neurotropin inhibits lipid accumulation by maintaining mitochondrial function in hepatocytes via AMPK activation. Front Physiol 11: 950, 2020.
62. Saum K, Campos B, Celdran-Bonafonte D, Nayak L, Sangwung P, Thakar C, Roy-Chaudhury P and Owens AP Iii PhD: Uremic advanced glycation end products and protein-bound solutes induce endothelial dysfunction through suppression of Krüppel-like factor 2. J Am Heart Assoc 7: e007566, 2018.
63. SenBanerjee S, Lin Z, Atkins GB, Greif DM, Rao RM, Kumar A, Feinberg MW, Chen Z, Simon DI, Luscinskas FW, *et al*: KLF2 is a novel transcriptional regulator of endothelial proinflammatory activation. J Exp Med 199: 1305-1315, 2004.
64. Guo D, Hildebrandt IJ, Prins RM, Soto H, Mazzotta MM, Dang J, Czernin J, Shyy JY, Watson AD, Phelps M, *et al*: The AMPK agonist AICAR inhibits the growth of EGFRvIII-expressing glioblastomas by inhibiting lipogenesis. Proc Natl Acad Sci USA 106: 12932-12937, 2009.
65. Viglino C, Foglia B and Montessuit C: Chronic AICAR treatment prevents metabolic changes in cardiomyocytes exposed to free fatty acids. Pflugers Arch 471: 1219-1234, 2019.
66. Hu L, Su L, Dong Z, Wu Y, Lv Y, George J and Wang J: AMPK agonist AICAR ameliorates portal hypertension and liver cirrhosis via NO pathway in the BDL rat model. J Mol Med (Berl) 97: 423-434, 2019.
67. Yu H, Liu Q, Chen G, Huang L, Luo M, Lv D and Luo S: SIRT3-AMPK signaling pathway as a protective target in endothelial dysfunction of early sepsis. Int Immunopharmacol 106: 108600, 2022.
68. Li JM, Lu W, Ye J, Han Y, Chen H and Wang LS: Association between expression of AMPK pathway and adiponectin, leptin, and vascular endothelial function in rats with coronary heart disease. Eur Rev Med Pharmacol Sci 24: 905-914, 2020.
69. Jia Q, Shi S, Yuan G, Shi J, Shi S, Wei Y and Hu Y: The effect of nicorandil in patients with cardiac syndrome X: A meta-analysis of randomized controlled trials. Medicine (Baltimore) 99: e22167, 2020.
70. Zhu H, Xu X, Fang X, Zheng J, Zhao Q, Chen T and Huang J: Effects of the antianginal drugs ranolazine, nicorandil, and ivabradine on coronary microvascular function in patients with nonobstructive coronary artery disease: A meta-analysis of randomized controlled trials. Clin Ther 41: 2137-2152.e12, 2019.
71. Abdelzaher WY, Khalaf HM, El-Hussieny M, Bayoumi A, Shehata S and Refaie M: Role of nitric oxide donor in methotrexate-induced testicular injury via modulation of pro-inflammatory mediators, eNOS and P-glycoprotein. Hum Exp Toxicol 39: 1700-1709, 2020.
72. Harb IA, Ashour H, Sabry D, El-Yasergy DF, Hamza WM and Mostafa A: Nicorandil prevents the nephrotoxic effect of cyclosporine-A in albino rats through modulation of HIF-1α/VEGF/eNOS signaling. Can J Physiol Pharmacol 99: 411-417, 2021.
73. Ishibashi Y, Takahashi N, Tokumaru A, Karino K, Sugamori T, Sakane T, Yoshitomi H, Sato H, Oyake N, Murakami Y and Shimada T: Effects of long-term nicorandil administration on endothelial function, inflammation, and oxidative stress in patients without coronary artery disease. J Cardiovasc Pharmacol 51: 311-316, 2008.

74. Refaie MMM, Shehata S, El-Hussieny M, Abdelraheem WM and Bayoumi AMA: Role of ATP-sensitive potassium channel (K_{ATP}) and eNOS in mediating the protective effect of nicorandil in cyclophosphamide-induced cardiotoxicity. Cardiovasc Toxicol 20: 71-81, 2020.
75. Sun X, Pan H, Tan H and Yu Y: High free fatty acids level related with cardiac dysfunction in obese rats. Diabetes Res Clin Pract 95: 251-259, 2012.
76. Fatahi S, Kord-Varkaneh H, Talaei S, Mardali F, Rahmani J, Ghaedi E, Tan SC and Shidfar F: Impact of phytosterol supplementation on plasma lipoprotein(a) and free fatty acid (FFA) concentrations: A systematic review and meta-analysis of randomized controlled trials. Nutr Metab Cardiovasc Dis 29: 1168-1175, 2019.
77. Smart NA, King N, McFarlane JR, Graham PL and Dieberg G: Effect of exercise training on liver function in adults who are overweight or exhibit fatty liver disease: A systematic review and meta-analysis. Br J Sports Med 52: 834-843, 2018.
78. Henderson GC: Plasma free fatty acid concentration as a modifiable risk factor for metabolic disease. Nutrients 13: 2590, 2021.